



SHORT COMMUNICATION

**Synthesis of LiFePO<sub>4</sub> nanocrystals and their properties as cathodic material for lithium ion batteries**

VADYM A. GALAGUZ, SERGIY M. MALOVANYI and EDUARD V. PANOV\*

*V.I. Vernadsky Institute of General and Inorganic Chemistry of the National Academy of Sciences of Ukraine, 32-34 Acad. Palladina Ave., Kyiv, 03680, Ukraine*

(Received 28 October 2017, revised 3 April, accepted 4 April 2018)

**Abstract:** The method of lithium iron phosphate (LiFePO<sub>4</sub>) synthesis in a melt mixture of choline chloride and diethylene glycol (DEG) at 230 °C is proposed. Powders with lamellar morphology consisting of LiFePO<sub>4</sub> crystals (size ~30 nm) with olivine structure were synthesized. The size of crystals increased to ~60 nm during the annealing process carried out to obtain a carbon coating on the grain surface of LiFePO<sub>4</sub>. The charge-discharge curves of the electrode prepared from these powders have a horizontal portion at the potential of 3.4 and 3.5 V, corresponding to the intercalation/deintercalation of lithium in the structure of olivine. The specific discharge capacity of the LiFePO<sub>4</sub>/C is 133 mA h g<sup>-1</sup> for a discharge current of 0.1C. The dependence of the anodic (cathodic) voltammetric current peaks,  $I_p$ , on the potential scan rate indicates the diffusion nature of the lithiating step. For the anodic and cathodic processes the averaged diffusion coefficient values are  $1.3 \times 10^{-10}$  and  $1.5 \times 10^{-10}$  cm<sup>2</sup> s<sup>-1</sup>, respectively.

**Keywords:** lithium ion batteries; cathode; polyol process.

INTRODUCTION

Lithium iron phosphate (LiFePO<sub>4</sub>) is one of the most effective materials for a cathode of commercial lithium-ion batteries.<sup>1</sup> However, the low electron conductivity and the Li<sup>+</sup> diffusion coefficient are the main lacks which prevent the commercialization of this material.<sup>1-5</sup> This lacks can be minimized by forming the grain microstructure of LiFePO<sub>4</sub> in order to reduce the path of diffusion for Li<sup>+</sup> and the contact electroresistance between the grains. The first lack is possibly due to the transition to nano-sized LiFePO<sub>4</sub>, and the second one to the carbon coating of LiFePO<sub>4</sub> particles. Despite the large number of studies aimed at improving the LiFePO<sub>4</sub> characteristics using the above-mentioned techniques, this problem is not fully resolved.<sup>1-9</sup> This prompted us to propose a low-temperature

\* Corresponding author. E-mail: vgalaguz@ukr.net  
<https://doi.org/10.2298/JSC171028036G>

synthesis method, which allows to obtain the nanocrystalline LiFePO<sub>4</sub> with the olivine structure at once, by passing the stage of long-term high-temperature (700–800 °C, 12–24 h) annealing. Usually, glucose or sucrose is used as a carbon source.<sup>9</sup> It is known that carboxylic acids have lower temperature of melting and decomposition, which allow to reduce the time and temperature of annealing. Also at the pyrolysis of carboxylic acids a little water is formed that may be the cause of the oxidation of nanopowders.<sup>10</sup> The carboxylic acids are good reducing agents because during the process of decomposition the organic acid molecule forms CO as the main reducing intermediate, which consequently leads to H<sub>2</sub> production.<sup>11</sup> So we suggested that it is expedient to use carboxylic acids.

## EXPERIMENTAL

The following analytical reagents were used in the synthesis of phosphates: NH<sub>4</sub>H<sub>2</sub>PO<sub>4</sub>, (NH<sub>4</sub>)<sub>2</sub>HPO<sub>4</sub>, FeSO<sub>4</sub>·7H<sub>2</sub>O, (NH<sub>4</sub>)<sub>2</sub>Fe(SO<sub>4</sub>)<sub>2</sub>·6H<sub>2</sub>O, NH<sub>4</sub>FePO<sub>4</sub>, CH<sub>3</sub>COOLi, choline chloride, 2,2'-oxydi(ethan-1-ol) (DEG) and malic acid. For the synthesis of the NH<sub>4</sub>FePO<sub>4</sub>·2H<sub>2</sub>O, necessary for the production of LiFePO<sub>4</sub>, we have developed and optimized the procedure for the interaction of ammonium phosphate with ferrous sulfate, in the presence of acetate or formate buffer solutions. FeSO<sub>4</sub>·7H<sub>2</sub>O or (NH<sub>4</sub>)<sub>2</sub>Fe(SO<sub>4</sub>)<sub>2</sub>·6H<sub>2</sub>O, (NH<sub>4</sub>)<sub>2</sub>HPO<sub>4</sub> and NH<sub>4</sub>H<sub>2</sub>PO<sub>4</sub> were taken as starting materials. The purity of synthesized NH<sub>4</sub>FePO<sub>4</sub> was confirmed by the X-ray diffraction analysis (XRD), showing no reflexes of any impurities in the diffractogram (JCPDS No. 00-45-0424).

The obtaining of lithium iron phosphate was based on the interaction of NH<sub>4</sub>FePO<sub>4</sub> with CH<sub>3</sub>COOLi in the liquid phase medium of the melt of choline chloride and DEG. Synthesis was carried out in a quartz reactor in argon medium for 1–8 h at 230 °C. The reactor was placed in an electric furnace with a programmable heating/cooling regime. The precipitate was washed in the distilled water and ethanol, separated by centrifugation and dried. The resulting powder was wetted with a solution of malic acid, dried and annealed (650 °C) for 1 h to obtain a carbon coating on the grain surface of LiFePO<sub>4</sub>.

Energy-dispersive X-ray spectroscopy (EDX) and X-ray diffraction (performed by DRON-4) were used to identify the elemental and phase composition of the samples. In order to study morphology and dispersion a scanning and transmission electron microscopy were used. These measurements were conducted by a JSM 2010 (TEM) and JEOL JSM 6060LA (SEM) with JED-2300 module (for X-ray spectroscopy). To measure the cyclic voltammograms and charge–discharge galvanostatic characteristics of the LiFePO<sub>4</sub>/C cathode, we used a potentiostat–galvanostat (Autolab-30 PGSTAT 302N) with two-electrode T-shaped teflon cell with a separator, and an auxiliary electrode which is also a reference electrode made of metallic lithium. Cycling of the LiFePO<sub>4</sub>/C cathode was performed in the potential range of 2.4–3.9 V.

From the LiFePO<sub>4</sub>/C powders obtained after annealing, a cathode mass was prepared having the following composition: LiFePO<sub>4</sub>/C (80 wt. %), polyvinylidene difluoride (PVDF) solution in 1-methyl-2-pyridone (10 wt. %), acetylene black (10 wt. %). From the cathode mass on the substrates made of stainless steel ( $S = 1 \text{ cm}^2$ ), the film LiFePO<sub>4</sub>/C electrodes were formed. The working electrode, after drying, was tested in a cell with a Li anode, an electrolyte from a 0.6 M solution of lithium bis(oxalato)borate (LiBOB) in an equimolar mixture of ethylene carbonate (EC) and dimethyl carbonate (DMC).

## RESULTS AND DISCUSSION

According to XRD data (Fig. 1), the obtained LiFePO<sub>4</sub> is characterized by good crystallinity after the first hour of synthesis. There are no impurities (within the sensitivity of the XRD method, all reflections are consistent with JCPDS No. 00-40-1499). Annealing of the synthesized sample of LiFePO<sub>4</sub> with malic acid (650 °C, 1 h) yields another product: the crystal size varies from ~30 (synthesized product) to ~60 nm (after annealing).

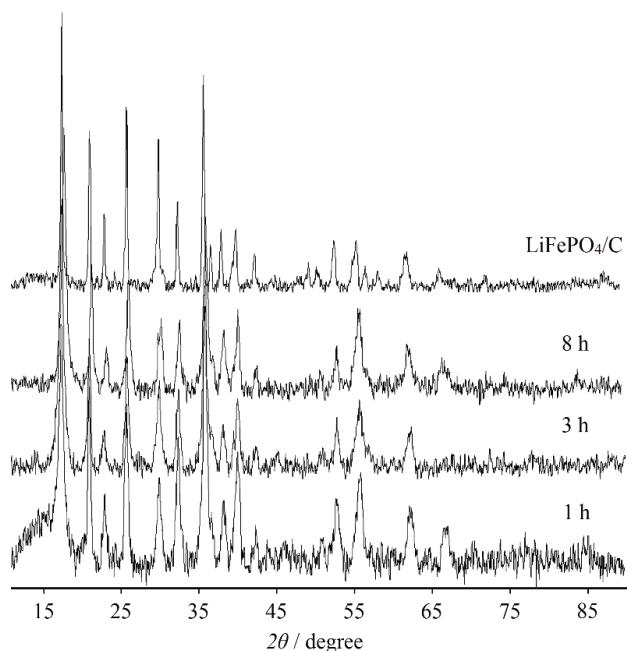


Fig. 1. X-ray diffraction patterns of the LiFePO<sub>4</sub> powder synthesized in the melt of choline chloride-DEG (1, 3 and 8 h) and LiFePO<sub>4</sub>/C composite after annealing.

Synthesized powders have lamellar morphology, which is related to the nature of the precursor NH<sub>4</sub>FePO<sub>4</sub>·2H<sub>2</sub>O.<sup>9</sup> This precursor was synthesized in the form of plates, a few microns in length and few tens of nanometers in thickness. In the process of exchange reaction with the lithium acetate, NH<sub>4</sub>FePO<sub>4</sub>·2H<sub>2</sub>O is broken down into smaller particles consisting of the LiFePO<sub>4</sub> nanocrystals (Fig. 2).

According to the data of the EDX analysis, the elemental composition of the synthesized material corresponds to the LiFePO<sub>4</sub> stoichiometry, the carbon content for various samples of the composite varies in the range of ~20 wt. %. This is more than the amount of theoretically expected carbon as a result of the pyrolysis of the crystals of malic acid on the surface of LiFePO<sub>4</sub>. It can be due to the presence of carbonized choline chloride residues and DEG in synthesized LiFePO<sub>4</sub>.

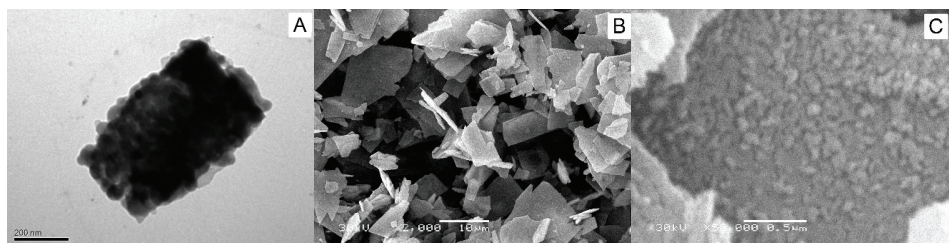


Fig. 2. TEM image (A) of the sample of  $\text{LiFePO}_4/\text{C}$  and SEM images (B and C) of the sample of  $\text{LiFePO}_4$ .

The electrochemical properties of the synthesized cathode material were estimated from the cyclic voltammetry (CV) data at a potential scan rate of 0.1, 0.2, 0.5 and 1  $\text{mV s}^{-1}$  in the potential range of 2.4–3.9 V (vs.  $\text{Li}^+/\text{Li}$  electrode, Fig. 3), as well as from the stationary charge–discharge characteristics (Fig. 4). On the charge–discharge curve, a plateau is observed in the potential range 3.4–3.5 V (vs.  $\text{Li}^+/\text{Li}$ ), responsible for the intercalation/deintercalation of the lithium into the structure of olivine. When the  $\text{LiFePO}_4/\text{C}$  composite is cycled for 25 cycles and the discharge current density increases from 0.1C to 2C, the capacity of the sample drops from 133 to 62  $\text{mA h g}^{-1}$ . The capacity was calculated per mass of active material.

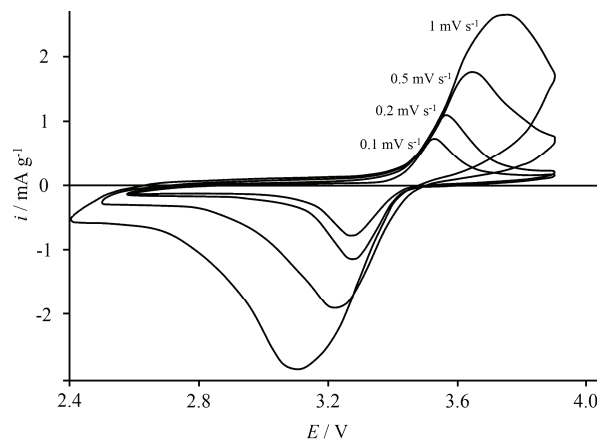


Fig. 3. Cyclic voltammograms of the  $\text{LiFePO}_4/\text{C}$  electrode in 0.6 M LiBOB in the EC:DMC (1:1) at potential sweep rates of 0.1, 0.2, 0.5 and 1  $\text{mV s}^{-1}$ .

The graph  $I_p - v^{1/2}$  (Fig. 5) is plotted at peak values of current ( $I_p$ ) of the CV curves at different potential scanning speeds  $v$ . Its form (straight line) indicates the reversibility of the electrode process. For this case, the Randles–Sevcik equation can be used to determine the diffusion  $D_{\text{Li}}$  coefficient:<sup>12,13</sup>

$$I_p = 2.99 \times 10^5 (\alpha n)^{1/2} A \Delta c D_{\text{Li}}^{1/2} v^{1/2} \quad (1)$$

here  $\alpha$  – the transfer coefficient,  $n$  – the number of transferred electrons,  $c$  – the initial concentration of vacant sites in the intercalate for the cathodic process,  $A$  – the electrode area.

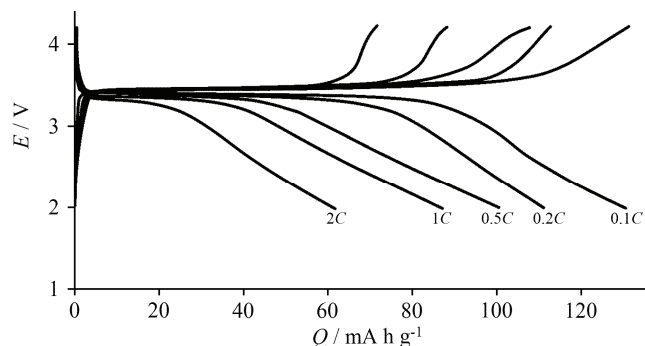


Fig. 4. Charge–discharge profiles of the LiFePO<sub>4</sub>/C electrode in 0.6 M LiBOB in the EC:DMC (1:1) at the current density of 0.1C, 0.2C, 0.5C, 1C and 2C.

The averaged apparent diffusion coefficients for lithium ions, calculated according to Eq. (1), were  $1.3 \times 10^{-10}$  and  $1.5 \times 10^{-10} \text{ cm}^2 \text{ s}^{-1}$  for the anodic and cathodic processes, respectively. Our results are somewhat inaccurate, because the Li insertion/deinsertion into/from LiFePO<sub>4</sub> did not fit the process at metal/liquid electrolyte boundary, implied by the Randles–Sevcik equation. We also used the geometric surface instead of the real one, that can lead to the overstatement of results. At the same time, the classic BET method can overestimate the real specific surface. A method based on the average diameter of the particles may to some extent underestimate a certain surface area, for example, when the LiFePO<sub>4</sub> particles have a porous texture. Despite these disadvantages, the calculation of diffusion coefficient following this equation is widely used.<sup>13</sup>

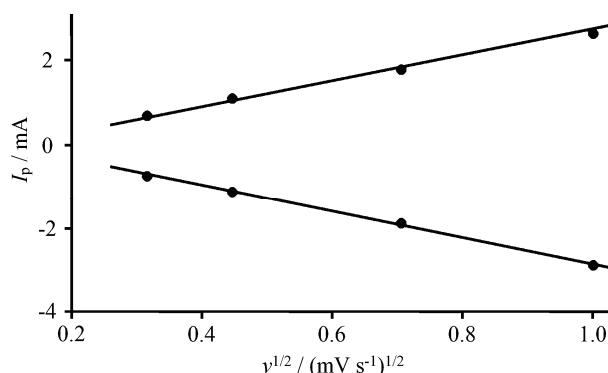


Fig. 5. Dependence of the anodic and cathodic current peaks of the LiFePO<sub>4</sub>/C electrode voltammograms in the 0.6 M LiBOB in EC:DMC (1:1) on the potential sweep rate.

## CONCLUSION

The synthesis of LiFePO<sub>4</sub> in the melt mixture of choline chloride and diethylene glycol at the 230 °C makes it possible to obtain the crystalline powders of the LiFePO<sub>4</sub> with the olivine structure and the average particle size of ~30 nm. After carbonization of the carbon precursor (malic acid), particles of the LiFePO<sub>4</sub>/C composite on the surface of the obtained powders increase to ~60 nm. The electrodes made from synthesized powders are characterized by the reversibility of the lithium incorporation/extraction process. The magnitudes of the averaged apparent diffusion coefficient for lithium ions are  $1.3 \times 10^{-10}$  and  $1.5 \times 10^{-10}$  cm<sup>2</sup> s<sup>-1</sup> for the anodic and cathodic processes, respectively. When the discharge current density increases from 0.1C to 2C, the sample capacity drops from 133 to 62 mA h g<sup>-1</sup>.

## ИЗВОД

СИНТЕЗА НАНОКРИСТАЛА LiFePO<sub>4</sub> И ЊИХОВЕ ОСОБИНЕ КАО КАТОДНОГ МАТЕРИЈАЛА ЗА ЛИТИЈУМ-ЈОН БАТЕРИЈЕ

VADYM A. GALAGUZ, SERGIY M. MALOVANYI и EDUARD V. PANOV

V.I. Vernadsky Institute of General and Inorganic Chemistry of the National Academy of Sciences of Ukraine,  
32-34 Acad. Palladina Ave., Kyiv, 03680, Ukraine

Предложена је метода синтезе литијум–гвожђе–фосфата (LiFePO<sub>4</sub>) у растопу холин-хлорида и диетилен-гликола на 230 °C. Нађено је да су синтетисани прахови ламеларне морфологије и да се састоје од кристала LiFePO<sub>4</sub> величине ~30 nm са структуром оливина. Величина кристала је расла до ~60 nm током анилирања чија је сврха била формирање угљеничног омотача на површини зрна LiFePO<sub>4</sub>. Криве пуњења и пражњења електроде која је направљена од оваквог праха је имала хоризонтални део у интервалу потенцијала 3,4–3,5 V, што одговара интеркалацији/деинтеркалацији литијума у структуру оливина. Специфични капацитет пражњења LiFePO<sub>4</sub>/C је износио 133 mA h g<sup>-1</sup> при струји пражњења од 0,1C. Зависност висине волтаметријских анодних и катодних струјних пикова од брзине линеарне промене потенцијала је указала да је ступањ литијације дифузиона-контролисан. Средње вредности првидних коефицијента дифузије литијумових јона у анодном и катодном процесу износе  $1.3 \times 10^{-10}$  и  $1.5 \times 10^{-10}$  cm<sup>2</sup> s<sup>-1</sup>, редом.

(Примљено 28. октобра 2017, ревидирано 3. априла, прихваћено 4. априла 2018)

## REFERENCES

1. A. K. Padhi, K. S. Nanjundaswamy, J. B. Goodenough, *J. Electrochem. Soc.* **144** (1997) 1188
2. N. Nitta, F. Wu., J. Lee, G. Yushin, *Mater. Today* **18** (2015) 252
3. C. Julien, A. Mauger, A. Vijh, K. Zaghib, *Lithium Batteries: Science and Technology*, Springer, New York, 2015, pp. 201–204
4. J. Speirs, M. Contestabile, Y. Houari, R. Gross, *Renew. Sustain. Energy Rev.* **35** (2014) 183
5. Z. Li, D. Zhang, F. Yang, *J. Mater. Sci.* **44** (2009) 2435
6. R. Malik, D. Burch, M. Bazant, G. Ceder, *Nano Lett.* **10** (2010) 4123
7. M. Gaberscek, R. Dominko, J. Jamnik, *Electrochim. Commun.* **9** (2007) 2778
8. T. V. Satyavani, A. K. Srinivas, P. S. Subba Rao, *Eng. Sci. Technol. Int. J.* **19** (2016) 178

9. W. Chunyang, X. Jian, C. Gaoshao, Z. Xinbing, Z. Shichao, *Cryst. Eng. Commun.* **16** (2014) 2239
10. Z. Yang, Y. Dai, S. Wang, J. Yub *J. Mater. Chem., A* **4** (2016) 18210
11. K. Kim, Y. H. Cho, D. Kam, H. S. Kim, J. W. Lee, *J. Alloys Compd.* **504** (2010) 166
12. Y. W. Denis, C. Fietzek, W. Weydanz, K. Donoue, T. Inoue, H. Kurokawa, S. Fujitania, *J. Electrochem. Soc.* **154** (2007) 253
13. M. Vujković, I. Stojković, N. Cvjetičanin, S. Mentus, *Electrochim. Acta* **92** (2013) 248.